

Department of Mathematics

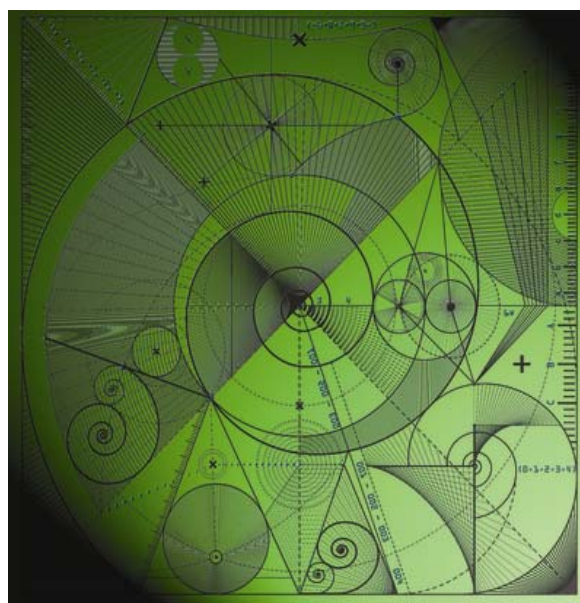
Preprint MPS_2010-05

18 March 2010

Numerical estimation of coercivity
constants for boundary integral operators in
acoustic scattering

by

T. Betcke and E.A. Spence



NUMERICAL ESTIMATION OF COERCIVITY CONSTANTS FOR BOUNDARY INTEGRAL OPERATORS IN ACOUSTIC SCATTERING

T. BETCKE* AND E.A. SPENCE†

Abstract. Coercivity is an important concept for proving existence and uniqueness of solutions to variational problems in Hilbert spaces. But, while the existence of coercivity estimates is well known for many variational problems arising from partial differential equations, it is still an open problem in the context of boundary integral operators arising from acoustic scattering problems, where rigorous coercivity results have so far only been established for combined integral operators on the unit circle and sphere. The main motivation for investigating coercivity in this context is that it has the potential to give error estimates for the Galerkin method which are explicit in the wavenumber k . One way to interpret coercivity is by considering the numerical range of the operator. The numerical range is a well established tool in spectral theory and algorithms exist to approximate the numerical range of finite dimensional matrices. We can therefore use Galerkin projections of the boundary integral operators to approximate the numerical range of the original operator. We prove convergence estimates for the numerical range of Galerkin projections of a general bounded linear operator on a Hilbert space to justify this approach. By computing the numerical range of the combined integral operator in acoustic scattering for several interesting convex, nonconvex, smooth and polygonal domains, we numerically study coercivity estimates for varying wavenumbers. Surprisingly, it turns out that for many domains a coercivity result seems to hold independently of the wavenumber or with only a mild dependence on it. Finally, we consider a trapping domain, for which there exist resonances (also called scattering poles) very close to the real line, to demonstrate that coercivity for a certain wavenumber k seems to be strongly dependent on the distance to the nearest resonance.

Key words. numerical range, coercivity, boundary integral operators

AMS subject classifications. 45P05, 47A12, 65R20,

1. Introduction. Let \mathcal{H} be a Hilbert space and $t : \mathcal{H} \times \mathcal{H} \rightarrow \mathbb{C}$ a sesquilinear form on \mathcal{H} . A standard variational problem is to find $u \in \mathcal{H}$ such that

$$t(u, v) = f(v), \quad \forall v \in \mathcal{H} \tag{1.1}$$

for a given $f \in \mathcal{H}'$, the dual space of \mathcal{H} . It is a classical result that there exists a unique solution to this problem if there are $C, \gamma > 0$ such that

$$|t(u, v)| \leq C \|u\| \|v\|, \quad \forall u, v \in \mathcal{H} \text{ (Continuity)}, \tag{1.2}$$

$$\gamma \|u\|^2 \leq |t(u, u)|, \quad \forall u \in \mathcal{H} \text{ (Coercivity)}. \tag{1.3}$$

Furthermore, if $u^{(h)}$ is a Galerkin solution of (1.1) in a finite dimensional subspace $\mathcal{V}^{(h)} \subset \mathcal{H}$ then Céa's Lemma [9] gives

$$\|u - u^{(h)}\| \leq \frac{C}{\gamma} \inf_{v \in \mathcal{V}^{(h)}} \|u - v\|. \tag{1.4}$$

Hence, the stability of the Galerkin approximation $u^{(h)}$ can be determined by the continuity constant C and the coercivity constant γ .

While estimates for C and γ are known for variational formulations of several classical PDEs they are still an open problem for boundary integral equation operators in acoustic scattering. Consider the problem of time-harmonic acoustic scattering from a sound-soft bounded obstacle $\Omega \subset \mathbb{R}^d$, ($d = 2, 3$) with Lipschitz boundary $\Gamma := \partial\Omega$. That is, we are looking for the solution u of the problem

$$\Delta u + k^2 u = 0 \quad \text{in } \mathbb{R}^d \setminus \overline{\Omega} \tag{1.5}$$

$$u = 0 \quad \text{on } \partial\Omega \tag{1.6}$$

$$\frac{\partial u_s}{\partial r} - iku_s = o(r^{-(d-1)/2}), \tag{1.7}$$

*Department of Mathematics, University of Reading, UK, t.betcke@reading.ac.uk Timo Betcke is supported by Engineering and Physical Sciences Research Council Grant EP/H004009/1.

†Department of Mathematics, University of Bath, UK, e.a.spence@bath.ac.uk. Euan Spence is supported by Engineering and Physical Sciences Research Council Grant EP/F06795X/1.

where $u = u_{inc} + u_s$ is the total field, u_{inc} is a solution of (1.5) in a neighborhood of Ω , such as an incident plane wave, u_s is the scattered field, and r is the radial coordinate. With the standard free-space Green's function defined as

$$\Phi(x, y) = \frac{i}{4} H_0^{(1)}(k|x-y|), \quad d = 2, \quad \Phi(x, y) = \frac{e^{ik|x-y|}}{4\pi|x-y|}, \quad d = 3,$$

for $x, y \in \mathbb{R}^d, x \neq y$, the solution u is given by

$$u(x) = u_{inc}(x) - \int_{\Gamma} \Phi(x, y) u_n(y) ds(y), \quad x \in \mathbb{R}^d \setminus \bar{\Omega},$$

where u_n is the outward pointing normal derivative of u . To compute u_n one can solve the boundary integral equation

$$A_{k,\eta} u_n = 2 \frac{\partial u_{inc}}{\partial n} - 2i\eta u_{inc} \quad (1.8)$$

with

$$A_{k,\eta} := I + K' - i\eta S, \quad (1.9)$$

where $\eta \in \mathbb{R} \setminus \{0\}$, I is the identity, and K' and S are defined by

$$K' u(x) := 2 \int_{\Gamma} \frac{\partial \Phi(x, y)}{\partial n(x)} u(y) ds(y), \quad S u(x) := 2 \int_{\Gamma} \Phi(x, y) u(y) ds(y), \quad x \in \Gamma.$$

Here, $n(x)$ is the outward pointing unit normal at Γ . The corresponding sesquilinear form is defined as $a_{k,\eta}(u, v) := \langle A_{k,\eta} u, v \rangle$, with $\langle u, v \rangle := \int_{\Gamma} u(y) \overline{v(y)} ds(y)$ being the standard L^2 -inner product. It was recently shown by Chandler-Wilde and Langdon in [14] that the operator $A_{k,\eta}$ is bijective with bounded inverse in the Sobolev spaces $H^{s-1/2}(\Gamma)$ for $|s| \leq \frac{1}{2}$ and $\eta \in \mathbb{R} \setminus \{0\}$ (see also the book by Colton and Kress [16] for unique solvability of (1.8) in $C(\Gamma)$ with C^2 boundary).

The common choice for the coupling parameter η is to take η proportional to k for k large, and η constant for k small. This has been based on theoretical studies for the case of Γ a circle or sphere [26, 25, 2, 3], and also on computational experience [10]. Recently this choice has been backed up as near optimal for conditioning for more general domains by the analysis of [13]. In this paper we will always assume that $\eta = k$ and therefore only write A_k instead of $A_{k,k}$. If k is clear from the context then for simplicity we just write A and $a(\cdot, \cdot)$ for the corresponding sesquilinear form. However, it is important to keep in mind that A and $a(\cdot, \cdot)$ are k -dependent.

In acoustic scattering continuity of $a(\cdot, \cdot)$ is much more easy to establish than coercivity. The key question is not only whether $a(\cdot, \cdot)$ is coercive, but also how γ depends on the wavenumber k . Indeed, this is the main motivation for studying the variational form of (1.8). The classical theory of second kind integral equations such as (1.8), which is based on the fact that for sufficiently smooth domains the operator (1.9) is a compact perturbation of the identity, gives quasi-optimal error estimates of the form (1.4) when the approximation space $\mathcal{V}^{(h)}$ consists of piecewise polynomials. However these error estimates have the following two disadvantages: The first is that they are not explicit in the wavenumber k ; i.e. they do not say how either the constant on the right hand side of (1.4), or the dimension of the approximation space N , depend on k [4]. The second is that much research effort has been focused recently on determining novel approximation spaces which take into account the high oscillation of the solution as k increases [12], and it does not appear that the classical theory can be used to prove error estimates for numerical methods using these subspaces. On the other hand, if continuity (1.2) and coercivity (1.3) of $a(\cdot, \cdot)$ can be established with constants C, γ explicit in k , then the error estimate (1.4) is valid for $\mathcal{V}^{(h)}$ any finite dimension subspace of L^2 . (There is the weaker theory of inf-sup constants for the variational problem (1.1) [9], [23], but this does not seem well-adapted to give k -explicit error estimates.)

A first result on the coercivity of $a(\cdot, \cdot)$ was given in [18], where it was shown that with Γ the unit circle (in 2-d) and the unit sphere (in 3-d) $a(\cdot, \cdot)$ is coercive for sufficiently large k with $\gamma \geq 1$. However, the question of coercivity and of k -dependence of γ is still unanswered for more complicated domains. In Section 2 we give an overview of existing coercivity results. To numerically estimate the coercivity constant on more complicated domains we use the close connection between coercivity and the numerical range of the operator A . The numerical range is defined as the set of all values $\langle Au, u \rangle$ in the complex plane with $u \in L^2(\Gamma)$, $\|u\| = 1$. It holds that $a(\cdot, \cdot)$ is coercive if and only if 0 is not in the closure of the numerical range. Hence, we can determine coercivity by computing the numerical range of the operator A , which is a well studied problem in the numerical linear algebra literature for matrices acting on \mathbb{C}^n . In Section 3 we describe some key properties of the numerical range, and in Section 4.1 we review a well known simple algorithm for computing the numerical range of an operator. Since in practice we need to work with Galerkin discretizations of $a(\cdot, \cdot)$ in Section 4.2, we give convergence estimates of the numerical range based on Galerkin discretizations with standard piecewise constant boundary element discretizations. In Section 5 we demonstrate numerically the convergence of the numerical range and use the numerical range computations to give numerical estimates of the coercivity constant for several interesting polygonal and smooth domains in two dimensions. We summarize our results and give conjectures about the coercivity constant in Section 6.

2. A summary of stability results for boundary integral operators in acoustic scattering. In this section we summarize the known continuity and coercivity results about the operator A , namely whether the inequalities (1.2) and (1.3) hold, and if so, how the constants C and γ depend on k . We note that these results also apply to the related operator:

$$A'_{k,\eta} := I + K - i\eta S \tag{2.1}$$

where K is the double layer potential

$$Ku(x) := 2 \int_{\Gamma} \frac{\partial \Phi(x, y)}{\partial n(y)} u(y) ds(y), \quad x \in \Gamma.$$

This operator appears in the classic indirect boundary integral formulation due to Brakhage and Werner [8], Leis [28] and Panić [33]. (“Indirect” refers to the fact that this integral operator does not arise from Green’s integral representation, whereas the so-called “direct” integral operator (1.9) does.) The operator $A'_{k,\eta}$ is the adjoint of $A_{k,\eta}$ with respect to the real inner product $\langle u, v \rangle_{\mathbb{R}} := \int_{\Gamma} u(y)v(y)ds(y)$. Thus

$$\|A_{k,\eta}\| = \|A'_{k,\eta}\|,$$

where the norm is that induced by the standard L^2 -inner product, and if the inequalities (1.2), (1.3) hold for $A_{k,\eta}$ then they also hold for $A'_{k,\eta}$ with the same C, γ .

Much less is known about coercivity (1.3) than continuity (1.2), so we discuss coercivity first. We then include a brief discussion of continuity results, for more comprehensive treatments see [13, 12]. In this section we will use the notation $D \lesssim E$ where D/E is less than a constant which is independent of k .

2.1. Coercivity. The only domains for which coercivity is completely understood is the circle (in 2-d) and sphere (in 3-d); this is because the operator A acts diagonally in the basis of trigonometric polynomials or spherical harmonics in 2 and 3-d respectively. For the circle, Domínguez, Graham and Smyshlyaev [18] showed that for the case $\eta = k$ coercivity holds for all sufficiently large k , with

$$\gamma \geq 1,$$

and for the sphere they proved

$$\gamma \geq 1 - \mathcal{O}(k^{-2/3}).$$

These difficult proofs relied on bounding below the eigenvalues of A , which are combinations of Bessel functions, uniformly in argument and order.

Although nothing is known directly about the coercivity constant γ for domains other than the circle/sphere, results on the norm of the inverse of A can be used to deduce information about γ using the fact that if A is coercive then

$$\gamma \leq \frac{1}{\|A^{-1}\|}.$$

This follows from (1.3) using Cauchy-Schwartz. Chandler-Wilde, Graham, Langdon and Linder [13] proved that if a part of Γ is C^1 then

$$\|A^{-1}\| \geq 1 \tag{2.2}$$

and hence

$$\gamma \leq 1. \tag{2.3}$$

Thus the bound obtained for γ for the circle in [18] is sharp. (2.2) follows from the fact that S and K are smoothing operators on smooth parts of Γ . In the same paper the authors constructed an example of a non-convex, non-starlike “trapping” domain in 2-d for which there exists an increasing sequence k_n where $\|A^{-1}\|$ grows as k_n increases. Indeed, for this domain, when $\eta = k$,

$$\|A^{-1}\| \gtrsim k_n^{9/10} \tag{2.4}$$

where B is independent of k . It is not known whether A is coercive for this domain or not, but this example shows that if it is coercive, it cannot be uniformly coercive in k since

$$\gamma \lesssim k_n^{-9/10}$$

which tends to zero as $k_n \rightarrow \infty$. A trapping domain to which this result applies is given in Section 5.3.

The final result on $\|A^{-1}\|$ which is relevant for coercivity was obtained by Chandler-Wilde and Monk in [15]. Their result implies that if Γ is Lipschitz, C^2 in a neighborhood of almost every $x \in \Gamma$, and starlike with respect to the origin, that is

$$\operatorname{ess\,inf}_{x \in \Gamma} x \cdot n(x) > 0,$$

then for $\eta \gtrsim k$

$$\|A^{-1}\| \lesssim 1.$$

Thus, the “blow-up” of $\|A^{-1}\|$ for the “trapping” domain in [13] cannot occur when Ω is starlike.

2.2. Continuity. By Cauchy-Schwartz, (1.2) holds for the bilinear form involving A with $C = \|A\|$, and this is seen to be sharp by letting $v = Au$. The question of bounding $\|A\|$ was investigated in detail in [13]. We summarise the main results below for the case $\eta = k$, noting that [13] obtains bounds explicit in both η and k .

In 2 and 3-dimensions, for Γ Lipschitz and piecewise C^1 , if k is sufficiently large,

$$1 \leq \|A\| \lesssim k^{(d-1)/2},$$

where d is the dimension. In 2-dimensions if Γ is piecewise C^2 there is an improved lower bound leading to

$$k^{1/3} \lesssim \|A\| \lesssim k^{1/2} \tag{2.5}$$

for sufficiently large k . In addition, in 2-d if Γ contains a straight line segment of length a then

$$\|A\| \gtrsim (ak)^{1/2} \tag{2.6}$$

for sufficiently large k , so that in this case the upper bound (2.5) is sharp in its k -dependence.

For the circle and sphere, the Fourier basis allows for bounds on $\|A\|$ to be obtained by bounding the eigenvalues of A , and this specialised method obtains sharper bounds than the general methods of [13]. For the circle and the sphere, when $\eta = k$ and k is sufficiently large,

$$\|A\| \lesssim k^{1/3}$$

[18]. (This result was obtained earlier for the sphere in the unpublished thesis [21].) Banjai and Sauter [5] recently obtained an improved bound on $\|A\|$ for the sphere: when k is sufficiently large

$$\|A\| \lesssim (1 + |\eta|k^{-2/3}).$$

This result, obtained partly by improved bounds on the eigenvalues, reduces to the earlier bound if $\eta = k$, but indicates that the norm of A is k -independent if $\eta = k^{2/3}$.

3. The numerical range and its connections to coercivity. In this section we discuss the connections between the numerical range of a bounded linear operator T on a Hilbert space with associated sesquilinear form $t(u, v) = \langle Tu, v \rangle$ and the coercivity constant γ . From (1.3) it follows that the largest possible coercivity constant γ is determined by

$$\gamma = \inf_{u \in \mathcal{H}} \frac{|t(u, u)|}{\|u\|^2}. \quad (3.1)$$

This value is closely related to the numerical range of T .

DEFINITION 3.1 (Numerical Range). *Let T be a bounded linear operator in a Hilbert space \mathcal{H} . The numerical range $W(T)$ is defined as the set*

$$W(T) = \{ \langle Tu, u \rangle, u \in \mathcal{H}, \|u\| = 1 \}.$$

The numerical range is also known under the name *field of values*. A beautiful summary of the numerical range and its connections to spectra and pseudospectra is given by Trefethen and Embree in [37]. Many results about the numerical range of linear operators in Hilbert spaces are contained in the book by Gustafson and Rao [22]. The numerical range has the following fundamental properties.

PROPOSITION 3.2 (Properties of the numerical range).

1. $W(T)$ is convex.
2. The spectrum $\sigma(T)$ is contained in the closure of $W(T)$
3. The closure of the numerical range of a normal operator is the convex hull of its spectrum $\sigma(T)$.

The proofs can be found in [22]. From the definition of the numerical range we have the following equivalent characterisation of coercivity.

PROPOSITION 3.3. *The sesquilinear form $t(u, v) := \langle Tu, v \rangle$ associated with a linear operator T on a Hilbert space is coercive if and only if $0 \notin W(T)$. Furthermore, if $t(\cdot, \cdot)$ is coercive then the coercivity constant γ is given by $\gamma = d(0, W(T))$, where d is the usual set distance.*

Proof. If $t(\cdot, \cdot)$ is coercive then, by definition, $0 < \inf_{u \in \mathcal{H} \setminus \{0\}} \frac{|\langle Tu, u \rangle|}{\langle u, u \rangle}$. Hence, $0 \notin \overline{W(T)}$.

On the other hand, if $t(\cdot, \cdot)$ is not coercive there exists a sequence $u^{(n)} \subset \mathcal{H} \setminus \{0\}$ such that $\frac{\langle Tu^{(n)}, u^{(n)} \rangle}{\langle u^{(n)}, u^{(n)} \rangle} \rightarrow 0$ for $n \rightarrow \infty$. Therefore, $0 \in \overline{W(T)}$. It follows immediately from (1.3) that $\gamma = d(0, W(T))$ if $t(\cdot, \cdot)$ is coercive. \square

This result allows us to rephrase the question of determining coercivity to the question of computing the numerical range $W(T)$. In fact, if T is normal then we immediately obtain from Proposition 3.2 the following characterisation.

PROPOSITION 3.4. *If T is normal then the associated sesquilinear form $t(\cdot, \cdot)$ is coercive if and only if 0 is not in the closed convex hull of the spectrum of T .*

An example is the operator $A_{k,\eta}$ defined in (1.8) on the unit circle.

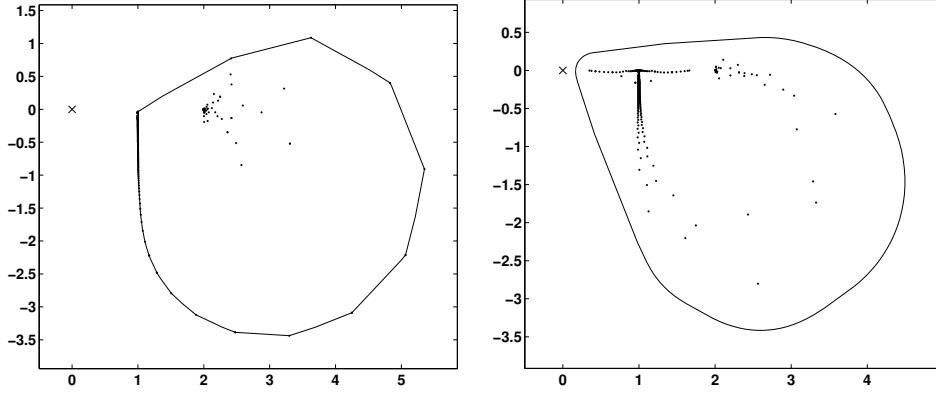


Fig. 3.1: Eigenvalues and boundary of the numerical range of the boundary integral operator $A_{k,\eta}$ on the unit circle (left plot) and on the equilateral triangle with side length 1 (right plot) for $k = \eta = 50$.

LEMMA 3.5. *If Γ is the boundary of the unit circle (in 2-d) or the unit sphere (in 3-d) then $A_{k,\eta}$ is normal.*

Proof. On the unit circle the integral operators K' and S and their adjoints diagonalise in the Fourier-basis $(e^{in\theta})_{n=-\infty\dots\infty}$. Hence, $A_{k,\eta}$ and $A_{k,\eta}^*$ commute. The standard way to prove the diagonalisation is to apply Green's theorem to $e^{in\theta}$ multiplied by an appropriate Bessel function [25, 26, 18], however the easiest way is to use the Fourier series representation of the fundamental solution,

$$H_0^{(1)}(k|re^{i\theta} - \rho e^{i\phi}|) = \sum_{n=-\infty}^{\infty} e^{in(\theta-\phi)} H_n^{(1)}(kr_>) J_n(kr_<), \quad (3.2)$$

where $r_> = \max(r, \rho)$, $r_< = \min(r, \rho)$, [1] equation (9.1.79), in the definitions of K' and S . The case of the sphere is similar, with spherical harmonics $Y_n^m(\hat{x})$ replacing the Fourier basis, and (3.2) replaced by

$$\frac{e^{ik|x-y|}}{4\pi|x-y|} = ik \sum_{n=0}^{\infty} j_n(kr_<) h_n^{(1)}(kr_>) Y_n^m(\hat{x}) \overline{Y_n^m(\hat{y})} \quad (3.3)$$

where $r_> = \max(|x|, |y|)$, $r_< = \min(|x|, |y|)$, [32] equation (11.3.44).

□

In the left plot of Figure 3.1 the boundary of the numerical range is shown for the operator $A_{k,\eta}$ on the unit circle with $k = \eta = 50$ (we explain how this was computed in Section 4.1). The black dots are the eigenvalues of the Galerkin discretization used for this computation. As expected the numerical range is the convex hull of the eigenvalues. Since on smooth curves Γ the operator $A_{k,\eta}$ is a compact perturbation of the identity the point 1 is the limit point of $\sigma(A)$, which is visible in the plot. Interestingly, some eigenvalues also seem to cluster around 2.

Let us now consider a more interesting domain. In the right plot of Figure 3.1 we show the eigenvalues and the numerical range for the operator $A_{k,\eta}$ on the boundary of an equilateral triangle with side length 1 and $k = \eta = 50$. Two observations are of interest. First of all, the numerical range is again bounded away from zero. Hence, the associated sesquilinear form is coercive for this k . Second, the numerical range is not the convex hull of the eigenvalues any more. This shows that the corresponding operator $A_{k,\eta}$ is not normal, and, as a consequence, that spectral information is not sufficient any more to determine whether the operator is coercive or not.

Characterisations of when $0 \in \overline{W(T)}$ were given by Burke and Greenbaum in [11]. They proved the following equivalence relation.

PROPOSITION 3.6. *Let T be a bounded linear operator. The following statements are equivalent:*

- (i) $0 \notin \overline{W(T)}$.
- (ii) *There exists $c \in \mathbb{C}$ such that $\overline{W(cT)}$ lies in the open right half plane.*
- (iii) $\min \{\|I - cT\| : c \in \mathbb{C}\} < 1$.

Statement (ii) is equivalent to the existence of $\alpha > 0$ and $c \in \mathbb{C}$, $|c| = 1$, such that $\operatorname{Re}\{\langle cTu, u \rangle\} \geq \alpha$ for all $u \in \mathcal{H}$. This is sometimes used instead of (1.3) as definition of coercivity. Statement (iii) as characterisation of coercivity has not been previously encountered by the authors. Its theoretical appeal is that it turns the question of proving coercivity of a bounded linear operator T into the question of estimating the norm of $I - cT$ for constants $c \in \mathbb{C}$.

The numerical range is not only of interest for the estimation of coercivity constants. It tells us much more about an operator. Let $r(T) := \sup\{|z| : z \in W(T)\}$ be the *numerical radius* of T . The numerical radius of T is equivalent to $\|T\|$ since

$$r(T) \leq \|T\| \leq 2r(T). \quad (3.4)$$

(see [22, Theorem 1.3-1]). The lower and upper bound are sharp. This result together with (3.1) allows us to formulate C ea's Lemma (1.4) purely using the numerical range.

THEOREM 3.7 (C ea's Lemma). *Let T be a bounded and coercive linear operator, $\mathcal{V}^{(h)}$ a subspace of \mathcal{H} and $W(T)$ the numerical range of T . Then for the Galerkin solution $u^{(h)}$ of (1.1) in the subspace $\mathcal{V}^{(h)}$ we have the estimate*

$$\|u - u^{(h)}\| \leq 2d(T) \inf_{v \in \mathcal{V}^{(h)}} \|u - v\|,$$

where $d(T) := \frac{\sup_{z \in W(T)} |z|}{\inf_{z \in W(T)} |z|}$.

The numerical range is also of practical interest for matrix iterations. For example, bounds for the convergence of GMRES applied to T can be formulated based on the numerical range [19, 20]. Hence, it is justified to study not only the coercivity and continuity constants γ and C separately but to consider the numerical range $W(T)$ itself. In particular, for boundary integral operators in acoustic scattering it is of interest to study the k -dependence of the numerical range.

4. Computing the numerical range. In Section 3 we showed that coercivity constants are determined by the distance of the numerical range to the origin. In this section we discuss the approximation of the numerical range. We start with the standard algorithm for computing the numerical range and then give a detailed convergence analysis given that we will be working with finite dimensional Galerkin approximations of the operator.

4.1. An algorithm for numerical range computations. Standard algorithms for computing the numerical range are based on the following principle. Let T be a bounded linear operator on a Hilbert space. We split up T as $T = T_H + iT_S$, where $T_H := \frac{1}{2}(T + T^*)$ and $T_S := \frac{1}{2i}(T - T^*)$. T_H is the self-adjoint (or Hermitian) part of T and iT_S is its skew-adjoint part. Then

$$\frac{\langle Tu, u \rangle}{\langle u, u \rangle} = \frac{\langle T_H u, u \rangle}{\langle u, u \rangle} + i \frac{\langle T_S u, u \rangle}{\langle u, u \rangle}.$$

Since T_H and T_S are self-adjoint, $\langle T_H u, u \rangle \in \mathbb{R}$ and $\langle T_S u, u \rangle \in \mathbb{R}$ for all $u \in \mathcal{H}$. It follows that the real part of all elements in the numerical range is determined by T_H . Hence, $W(T)$ is contained in the strip $\{z \in \mathbb{C} : h^{(m)} \leq \operatorname{Re}\{z\} \leq h^{(M)}\}$, where

$$h^{(m)} = \inf_{u \in \mathcal{H} \setminus \{0\}} \frac{\langle T_H u, u \rangle}{\langle u, u \rangle}, \quad h^{(M)} = \sup_{u \in \mathcal{H} \setminus \{0\}} \frac{\langle T_H u, u \rangle}{\langle u, u \rangle}. \quad (4.1)$$

By multiplying the operator T with $e^{i\theta}$ for $\theta \in [0, \pi]$ and computing $h^{(m)}$ and $h^{(M)}$ again we obtain a set of enclosing lines that characterise the convex set $W(T)$. Denote by $h_\theta^{(m)}$ and $h_\theta^{(M)}$ the left

and right bound for the numerical range $W(e^{i\theta}T)$ obtained as in (4.1). We have the following algorithm to compute the coercivity constant γ .

```

Input: Bounded linear operator  $T$ , Number of approximating points  $N$ 
Output: 0 or lower bound for coercivity constant  $\gamma$ 
1  $W := \mathbb{C}$ ;  $angles := \{\frac{j\pi}{N}, j = 0, \dots, N-1\}$ ;
2 foreach  $\theta \in angles$  do
3   | Compute  $h_\theta^{(m)}, h_\theta^{(M)}$ ;
4   |  $W := W \cap e^{-i\theta}\{z \in \mathbb{C} : h_\theta^{(m)} \leq \text{Re}\{z\} \leq h_\theta^{(M)}\}$ ;
5 end
6 if  $0 \notin W$  then
7   | return  $\gamma := d(0, W)$ ;
8 else
9   |  $\gamma := 0$ ;
10 end
11 return  $\gamma$ ;

```

Algorithm 1: Computation of coercivity constant γ

Algorithm 11 computes an enclosing domain $W \supset W(T)$ using N rotations of the original operator T . For $N \rightarrow \infty$ from the convexity of $W(T)$ it follows that $W \rightarrow \overline{W(T)}$. If $0 \notin W$ then the algorithm returns a positive lower bound for γ . Otherwise, either T is not coercive or N needs to be increased. If \mathcal{H} is finite dimensional, and therefore T a matrix, we can also directly compute points on the boundary of the numerical range and thereby give an interior approximation. Let $\lambda_{min}^{(\theta)}$ and $\lambda_{max}^{(\theta)}$ be the smallest, respectively largest, eigenvalue of the Hermitian part of $e^{i\theta}T$ with associated eigenvectors v_{min} and v_{max} . Then the corresponding points on the boundary of the numerical range of $W(T)$ are given by $p_{min}^{(\theta)} = \frac{\langle T v_{min}, v_{min} \rangle}{\langle v_{min}, v_{min} \rangle}$ and $p_{max}^{(\theta)} = \frac{\langle T v_{max}, v_{max} \rangle}{\langle v_{max}, v_{max} \rangle}$. It follows that the convex hull of all such points for different θ is a subset of $W(T)$, since $W(T)$ itself is convex. More information to numerical range computations can be found in [22]. An algorithm for estimating the numerical range of large and sparse matrices is described in [7].

If \mathcal{H} is infinite dimensional we approximate T from a finite dimensional basis $\{\chi_1, \dots, \chi_n\} \subset \mathcal{H}$ using a Galerkin approximation of T . The numerical range of T is then approximated by

$$W(T^{(h)}) = \left\{ \frac{x^H T^{(h)} x}{x^H M^{(h)} x}, x \in \mathbb{C}^n \setminus \{0\} \right\},$$

where $T^{(h)} = [\langle T \chi_i, \chi_j \rangle]$, $i, j = 1, \dots, n$ is the Galerkin projection of T and $M^{(h)} = [\langle \chi_i, \chi_j \rangle]$, the mass-matrix, is the corresponding projection of the identity in the finite dimensional basis. Hence, we need to solve generalized eigenvalue problems of the form

$$T^{(h)} \underset{H}{=} x = \lambda M^{(h)} x,$$

where $T^{(h)} \underset{H}{=}$ is the Hermitian part of $e^{i\theta}T^{(h)}$.

When solving integral equations using the Galerkin method with locally defined basis functions typically, at least in 2-d, the matrix $M^{(h)}$ has low bandwidth or is even diagonal. We therefore compute the Cholesky decomposition $M^{(h)} = CC^H$ to obtain the standard eigenvalue problem $C^{-1}T^{(h)} \underset{H}{=} C^{-H}y = \lambda y$ with $y = C^H x$. This is equivalent to changing to an orthonormal basis of the Galerkin subspace.

4.2. Convergence of the numerical range of a Galerkin discretization. In this section we analyse the convergence of the numerical range $W(T^{(h)})$ of a Galerkin discretisation $T^{(h)}$ to the numerical range of $W(T)$ for a sequence of subspaces $\mathcal{V}^{(h_0)} \subset \mathcal{V}^{(h_1)} \subset \dots \subset \mathcal{H}$, where h is usually interpreted as the fineness of a boundary element discretisation of an integral operator. The Galerkin discretisation $T^{(h)}$ is obtained by restricting the variational problem (1.1) on \mathcal{H} to a variational problem on a finite dimensional subspace $\mathcal{V}^{(h)} \subset \mathcal{H}$. From the definition of $T^{(h)}$

as Galerkin discretisation and the variational characterisation of the numerical range it follows immediately that

$$W(T^{(h)}) = \{\langle Tu, u \rangle : u \in \mathcal{V}^{(h)}, \|u\| = 1\} \subset W(T).$$

In this section we will use the notation $d(X, Y) := \inf\{|x - y| : x \in X, y \in Y\}$ for the distance of two sets. Correspondingly, $d(x, Y) := d(\{x\}, Y)$ is the distance of a single point x to the set Y . For the analysis we need the following perturbation Lemma.

LEMMA 4.1. *Let $z \in W(T)$ with associated $u \in \mathcal{H}$, $\|u\| = 1$, such that $z = \langle Tu, u \rangle$. Let $0 < \epsilon \leq 1$ and choose $\hat{u} \in \mathcal{H}$ with $\|u - \hat{u}\| \leq \epsilon$. Then*

$$\left| z - \frac{\langle T\hat{u}, \hat{u} \rangle}{\langle \hat{u}, \hat{u} \rangle} \right| \leq 8\|T\|\epsilon,$$

Proof. Let $f = u - \hat{u}$. Then $\|f\| \leq \epsilon$. We have

$$z = \langle T(\hat{u} + f), \hat{u} + f \rangle$$

and therefore

$$|z - \langle T\hat{u}, \hat{u} \rangle| \leq 2\|T\|\|\hat{u}\|\|f\| + \|T\|\|f\|^2. \quad (4.2)$$

We now estimate

$$\begin{aligned} |z - \langle T\hat{u}, \hat{u} \rangle| &\geq \left| z - \frac{\langle T\hat{u}, \hat{u} \rangle}{\langle \hat{u}, \hat{u} \rangle} \right| - \left| \langle T\hat{u}, \hat{u} \rangle - \frac{\langle T\hat{u}, \hat{u} \rangle}{\langle \hat{u}, \hat{u} \rangle} \right| \\ &\geq \left| z - \frac{\langle T\hat{u}, \hat{u} \rangle}{\langle \hat{u}, \hat{u} \rangle} \right| - \|T\| |1 - \|\hat{u}\|^2|. \end{aligned} \quad (4.3)$$

Combining this with (4.2) and using $|1 - \|\hat{u}\|^2| \leq 2\|f\| + \|f\|^2$ gives

$$\left| z - \frac{\langle T\hat{u}, \hat{u} \rangle}{\langle \hat{u}, \hat{u} \rangle} \right| \leq 2\|T\|\|f\| [\|\hat{u}\| + \|f\| + 1].$$

With $\|\hat{u}\| \leq \|u\| + \|f\| = 1 + \|f\|$ we have

$$\left| z - \frac{\langle T\hat{u}, \hat{u} \rangle}{\langle \hat{u}, \hat{u} \rangle} \right| \leq 2\|T\|\|f\| [2 + 2\|f\|] \leq 8\|T\|\epsilon$$

since $\|f\| \leq \epsilon \leq 1$. \square

We can now give a first convergence result. In order to state it we define the set $W_\epsilon(T) := \{z \in W(T) : d(z, \partial W(T)) \geq \epsilon\}$. Hence, for any $\epsilon > 0$ we have $W_\epsilon(T) \subset W(T)$ and $\lim_{\epsilon \rightarrow 0} d(z, W_\epsilon(T)) = 0 \forall z \in W(T)$. Also, by $\text{conv}\{z_1, \dots, z_M\} \subset \mathbb{C}$ we denote the closed convex hull of the points $z_1, \dots, z_M \in \mathbb{C}$.

THEOREM 4.2. *Let $\mathcal{V}^{(h_\epsilon)}$ be an asymptotically dense sequence of finite dimensional subspaces of \mathcal{H} such that $\mathcal{V}^{(h_0)} \subset \mathcal{V}^{(h_1)} \subset \dots \subset \mathcal{H}$. Denote by $T^{(h_\epsilon)}$ the associated Galerkin discretization of T . For any $\epsilon > 0$ there exists $m \in \mathbb{N}$ such that $W_\epsilon(T) \subset W(T^{(h_j)}) \subset W(T)$ for any $j \geq m$.*

Proof. Without restriction let $0 < \epsilon \leq 1$. The case of larger ϵ follows from this since $W_{\epsilon_1}(T) \subset W_{\epsilon_2}(T)$ for $\epsilon_1 \geq \epsilon_2$. Choose a finite number of M points z_j in $W(T) \setminus W_\epsilon(T)$ such that for $Z = \text{conv}\{z_1, \dots, z_M\}$ we have $W_\epsilon(T) \subset Z$ and $d(\partial W_\epsilon(T), \partial Z) > 0$. This is possible due to the convexity of $W(T)$. Now let $\delta > 0$ be small enough, such that for any set $Z_\delta = \text{conv}\{\hat{z}_1, \dots, \hat{z}_M\}$ with \hat{z}_j satisfying $|z_j - \hat{z}_j| \leq \delta$ it holds that $W_\epsilon(T) \subset Z_\delta$. Hence, perturbing the points z_j by at most δ still results in a convex set that encloses $W_\epsilon(T)$. Denote by $u_j \in \mathcal{H}$, $\|u_j\| = 1$, elements of \mathcal{H} associated with z_j such that $z_j = \langle Tu_j, u_j \rangle$ and choose $m \in \mathbb{N}$ sufficiently large such that there exists $\hat{u}_j \in \mathcal{V}^{(h_m)} \setminus \{0\}$ with $\|u_j - \hat{u}_j\| \leq \delta/(8\|T\|)$ for all $1 \leq j \leq M$. The existence of such an m follows from the asymptotic density of the subspaces $\mathcal{V}^{(h_\epsilon)}$ in \mathcal{H} . From Lemma 4.1 and the choice

of δ it follows now for the points $\hat{z}_j = \frac{\langle T\hat{u}_j, \hat{u}_j \rangle}{\langle \hat{u}_j, \hat{u}_j \rangle}$ that $W_\epsilon(T) \subset \text{conv}\{\hat{z}_1, \dots, \hat{z}_M\}$. Furthermore, from $\hat{z}_j \in W(T^{(h_m)})$ and the convexity of the numerical range we have $W_\epsilon(T) \subset W(T^{(h_m)})$ and due to the definition of the subspaces $\mathcal{V}^{(h_j)}$ also $W_\epsilon(T) \subset W(T^{(h_\ell)}) \subset W(T)$ for any $\ell \geq m$. \square

REMARK 4.3. *It follows from Theorem 4.2 that every point in the interior of $W(T)$ also belongs to the numerical range of a sufficiently fine Galerkin discretisation. Hence, the main difference between the numerical range of a Galerkin discretisation and that of the original operator T is the behaviour of their boundaries. Indeed, $T^{(h)}$ is finite dimensional, and hence $W(T^{(h)})$ is closed. However, $W(T)$ is in general neither open nor closed.*

We now prove a simple convergence estimate for the numerical range of a boundary integral operator based on a Galerkin boundary element discretization with piecewise constant elements of diameter h . To express the convergence result let $\Delta_\nu := \{z \in \mathbb{C} : |z| \leq \nu\}$. Also, for two sets $A, B \subset \mathbb{C}$ let $A + B := \{a + b : a \in A, b \in B\}$.

THEOREM 4.4. *Let Ω be a piecewise smooth Lipschitz domain with boundary Γ and $T : L^2(\Gamma) \rightarrow L^2(\Gamma)$ a bounded linear operator. Denote by $T^{(h)}$ its Galerkin discretisation from a space $\mathcal{V}^{(h)}$ of piecewise constant elements of diameter at most h . Then $W(T^{(h)}) \subset W(T)$ and for any $\epsilon > 0$ and $0 < \alpha \leq 1$ there exists $C > 0$, which depends on T , ϵ and α such that*

$$W_\epsilon(T) \subset W(T^{(h)}) + \Delta_{Ch^\alpha}.$$

Proof. As in the proof of Theorem 4.2 we choose M points in $W(T) \setminus W_\epsilon(T)$ such that $W_\epsilon(T) \subset Z := \text{conv}\{z_1, \dots, z_M\}$ and $d(\partial W_\epsilon(T), \partial Z) > 0$. Denote by $u_j \in L^2(\Gamma)$, $\|u_j\|_{L^2(\Gamma)} = 1$ functions associated with z_j , such that $z_j = \langle Tu_j, u_j \rangle$. Also, as in the proof of Theorem 4.2 let $\delta > 0$ be small enough such that for every $Z_\delta := \text{conv}\{\hat{z}_1, \dots, \hat{z}_M\}$ with $|z_j - \hat{z}_j| \leq \delta$ we have $W_\epsilon(T) \subset Z_\delta$.

Since Γ is a Lipschitz boundary, the Sobolev space $H^\alpha(\Gamma)$ is well defined for $0 < \alpha \leq 1$. Also, $H^\alpha(\Gamma)$ is dense in $L^2(\Gamma)$. Hence, there exist functions $\hat{u}_j \in H^\alpha(\Gamma) \setminus \{0\}$, such that $\|u_j - \hat{u}_j\|_{L^2(\Gamma)} \leq \delta / (8\|T\|_{L^2(\Gamma)})$. From Lemma 4.1 it now follows that $|z_j - \hat{z}_j| \leq \delta$ for $\hat{z}_j = \frac{\langle T\hat{u}_j, \hat{u}_j \rangle}{\langle \hat{u}_j, \hat{u}_j \rangle}$ and therefore $W_\epsilon(T) \subset \text{conv}\{\hat{z}_1, \dots, \hat{z}_M\}$.

Without restriction we now assume that the functions \hat{u}_j have been scaled to $\|\hat{u}_j\|_{L^2(\Gamma)} = 1$. By approximation results for piecewise constant basis functions [35] there exists $\hat{u}_j^{(h)} \in \mathcal{V}^{(h)}$ such that

$$\|\hat{u}_j - \hat{u}_j^{(h)}\|_{L^2(\Gamma)} \leq Ch^\alpha |\hat{u}_j|_{H^\alpha(\Gamma)}, \quad (4.4)$$

$j = 1, \dots, M$ for some $C > 0$ independent of j and h . Let $L := \max_j |\hat{u}_j|_{H^\alpha(\Gamma)}$. For the points $\hat{z}_j^{(h)} = \frac{\langle T\hat{u}_j^{(h)}, \hat{u}_j^{(h)} \rangle}{\langle \hat{u}_j^{(h)}, \hat{u}_j^{(h)} \rangle}$ it follows from Lemma 4.1 that $|\hat{z}_j - \hat{z}_j^{(h)}| \leq 8CL\|T\|h^\alpha$. Subsuming the constants in C we have

$$|\hat{z}_j - \hat{z}_j^{(h)}| \leq Ch^\alpha \quad (4.5)$$

for some $C > 0$. It follows that the boundary of the convex hull of the points \hat{z}_j and the boundary of the convex hull of the points $\hat{z}_j^{(h)}$ also have a distance bounded by Ch^α for some $C > 0$ and therefore, by the choice of the points \hat{z}_j

$$W_\epsilon(T) \subset \text{conv}\{\hat{z}_1, \dots, \hat{z}_M\} \subset \text{conv}\{\hat{z}_1^{(h)}, \dots, \hat{z}_M^{(h)}\} + \Delta_{Ch^\alpha}.$$

From the convexity of the numerical range we have $\text{conv}\{\hat{z}_1^{(h)}, \dots, \hat{z}_M^{(h)}\} \subset W(T^{(h)})$ giving

$$W_\epsilon(T) \subset W(T^{(h)}) + \Delta_{Ch^\alpha}.$$

The statement $W(T^{(h)}) \subset W(T)$ follows trivially from the variational characterisation of the numerical range. \square

REMARK 4.5. *Asymptotically, the rate of convergence in Theorem 4.4 is $O(h)$. However, in practice the constant C may be large if the \hat{u}_j are measured in the $H^1(\Gamma)$ norm. If \hat{u}_j is better*

represented in $H^\alpha(\Gamma)$ for some $\alpha < 1$ then we may numerically only see convergence of the rate $O(h^\alpha)$. However, for sufficiently small h the rate of convergence will eventually approach $O(h)$. An example is given in Section 5.1.

A slight improvement on the convergence rate of Theorem 4.4 can be obtained using properties of the Galerkin approximations. However, we will see that this only applies to the boundary integral operator A on domains which are smoother than just Lipschitz: we prove that $C^{2,\beta}$, $0 < \beta \leq 1$ is sufficient. In addition the operator must be self-adjoint, however this is not restrictive since, as shown earlier, we can compute $W(T)$ by only considering the Hermitian part T_H . We first prove a refinement of Lemma 4.1 in the case where \hat{u} is the Galerkin approximation of u .

LEMMA 4.6. *Let X be a continuous linear operator on \mathcal{H} which is self adjoint: $X^* = X$. Let $z \in W(X)$ with associated $u \in \mathcal{H}$, $\|u\| = 1$, such that $z = \langle Xu, u \rangle$. Let $\mathcal{V}^{(h)}$ be a finite dimensional subspace of \mathcal{H} , let $u^{(h)}$ denote the Galerkin approximation to u defined by*

$$\langle u^{(h)} - u, v^{(h)} \rangle = 0, \quad \forall v^{(h)} \in \mathcal{V}^{(h)}, \quad (4.6)$$

and suppose that

$$\|u - u^{(h)}\| \leq \frac{1}{2}\|u\|.$$

Then

$$\left| z - \frac{\langle u^{(h)}, Xu^{(h)} \rangle}{\langle u^{(h)}, u^{(h)} \rangle} \right| \leq 4\|u - u^{(h)}\| \left(\|Xu^{(h)} - (Xu^{(h)})^{(h)}\| + \|Xu - (Xu)^{(h)}\| + \|X\|\|u - u^{(h)}\| \right), \quad (4.7)$$

where $(Xu^{(h)})^{(h)}$ and $(Xu)^{(h)}$ are the Galerkin approximations of $Xu^{(h)}$ and Xu .

Proof. By the triangle inequality, Cauchy Schwartz, and the fact that $\|u - u^{(h)}\| \leq 1/2$ we have

$$\begin{aligned} \left| \langle u, Xu \rangle - \frac{\langle u^{(h)}, Xu^{(h)} \rangle}{\langle u^{(h)}, u^{(h)} \rangle} \right| &\leq \left| \frac{\langle u, Xu \rangle - \langle u^{(h)}, Xu^{(h)} \rangle}{\langle u^{(h)}, u^{(h)} \rangle} \right| + |\langle u, Xu \rangle| \left| \frac{1}{\langle u, u \rangle} - \frac{1}{\langle u^{(h)}, u^{(h)} \rangle} \right|, \\ &\leq \left| \frac{\langle u, Xu \rangle - \langle u^{(h)}, Xu^{(h)} \rangle}{\langle u^{(h)}, u^{(h)} \rangle} \right| + \|X\| \left| \frac{\langle u, u \rangle - \langle u^{(h)}, u^{(h)} \rangle}{\langle u^{(h)}, u^{(h)} \rangle} \right|, \\ &\leq 4 \left(|\langle u, Xu \rangle - \langle u^{(h)}, Xu^{(h)} \rangle| + \|X\| |\langle u, u \rangle - \langle u^{(h)}, u^{(h)} \rangle| \right). \end{aligned}$$

The result (4.7) now follows from the following two relations

$$\langle u, Xu \rangle - \langle u^{(h)}, Xu^{(h)} \rangle = \langle Xu^{(h)} - (Xu^{(h)})^{(h)}, u - u^{(h)} \rangle + \langle u - u^{(h)}, Xu - (Xu)^{(h)} \rangle \quad (4.8)$$

and

$$\langle u, u \rangle - \langle u^{(h)}, u^{(h)} \rangle = \langle u - u^{(h)}, u - u^{(h)} \rangle. \quad (4.9)$$

These are both consequences of the Galerkin property (4.6) and the fact that X is self-adjoint. Indeed

$$\begin{aligned} \langle u^{(h)}, Xu^{(h)} \rangle - \langle u, Xu \rangle &= \langle u^{(h)}, X(u^{(h)} - u) \rangle + \langle u^{(h)} - u, Xu \rangle \\ &= \langle Xu^{(h)}, u^{(h)} - u \rangle + \langle u^{(h)} - u, Xu \rangle \end{aligned}$$

by $X = X^*$, and using the property (4.6) to subtract off $(Xu^{(h)})^{(h)}$ and $(Xu)^{(h)}$ from the first and second brackets respectively yields (4.8). Property (4.6) also implies

$$\langle u^{(h)}, u^{(h)} \rangle = \langle u, u^{(h)} \rangle = \langle u^{(h)}, u \rangle$$

which gives (4.9). \square

The key point about equation (4.7) is that each term on the right hand side is the product of two errors in Galerkin approximations, thus the Galerkin approximation to the functional $\langle u, Xu \rangle$ converges faster than $\|u - u^{(h)}\|$ – this is an example of superconvergence. Another example of Galerkin approximations of functionals exhibiting superconvergence is given in [34].

Using Lemma 4.5 instead of Lemma 4.1 we can now prove a refined version of Theorem 4.4 for the numerical range of self-adjoint operators.

THEOREM 4.7. *Let Ω be a Lipschitz domain with boundary Γ and $X : L^2(\Gamma) \rightarrow L^2(\Gamma)$ a self-adjoint bounded linear operator which also maps $H^1(\Gamma)$ to $H^1(\Gamma)$. Denote by $X^{(h)}$ its Galerkin discretisation from a space $\mathcal{V}^{(h)} \subset L^2(\Gamma)$ of piecewise constant elements of diameter at most h . Then $W(X^{(h)}) \subset W(X)$ and for any $\epsilon > 0$ there exists h_0 and $C > 0$ (C depending on X , ϵ , and h_0), such that for all $h \leq h_0$*

$$W_\epsilon(X) \subset W(X^{(h)}) + \Delta_{Ch^2}.$$

Proof. This is identical to that of Theorem 4.4 for the case $\alpha = 1$ except that now Lemma 4.5 gives that

$$|\hat{z}_j - \hat{z}_j^{(h)}| \leq Ch^2$$

for some $C > 0$. The requirement that $X : H^1(\Gamma) \rightarrow H^1(\Gamma)$ is necessary to apply the interpolation result (4.4) to $X\hat{u}_j$ and $X\hat{u}_j^{(h)}$, and h_0 is chosen such that for all $h \leq h_0$

$$\|\hat{u}_j - \hat{u}_j^{(h)}\|_{L_2(\Gamma)} \leq \frac{1}{2}, \quad j = 1, \dots, M.$$

□

We now proof that the approximation of the numerical range of $A_{k,\eta}$ also shows superconvergence if Γ is sufficiently smooth. We need the following two lemmas.

LEMMA 4.8. *If Γ is $C^{2,\beta}$, $0 < \beta \leq 1$ then the operators $A_H := \frac{1}{2}(A_{k,\eta} + A_{k,\eta}^*)$, and $A_S := \frac{1}{2i}(A_{k,\eta} - A_{k,\eta}^*)$, where $A_{k,\eta}$ is given by (1.9) and $A_{k,\eta}^* = \overline{A'_{k,\eta}}$ where $A'_{k,\eta}$ is given by (2.1), map $L^2(\Gamma) \rightarrow L^2(\Gamma)$ and $H^1(\Gamma) \rightarrow H^1(\Gamma)$*

Proof. Certainly if S, K , and K' all map $L^2(\Gamma) \rightarrow L^2(\Gamma)$ and $H^1(\Gamma) \rightarrow H^1(\Gamma)$ then so do A_H and A_S . When Γ is Lipschitz

$$\begin{aligned} S &: H^{s-1/2}(\Gamma) \rightarrow H^{s+1/2}(\Gamma), \\ K' &: H^{s-1/2}(\Gamma) \rightarrow H^{s-1/2}(\Gamma), \\ K &: H^{s+1/2}(\Gamma) \rightarrow H^{s+1/2}(\Gamma) \end{aligned}$$

for $|s| \leq 1/2$, [29, Theorem 7.1]. Thus all three map $L^2(\Gamma) \rightarrow L^2(\Gamma)$, but only S and K map $H^1(\Gamma) \rightarrow H^1(\Gamma)$. By [17, Theorem 3.6], if Γ is $C^{2,\beta}$, $0 < \beta \leq 1$ then $K' : L^2(\Gamma) \rightarrow H^1(\Gamma)$ and thus maps $H^1(\Gamma) \rightarrow H^1(\Gamma)$. □

LEMMA 4.9. *Let Γ be $C^{2,\beta}$, $0 < \beta \leq 1$. Let $A_{k,\eta}^{(h)}$ be the Galerkin discretisation of $A_{k,\eta}$ from a space $\mathcal{V}^{(h)} \subset L^2(\Gamma)$ of piecewise constant elements of diameter at most h and denote by $u^{(h)} \in \mathcal{V}^{(h)}$ the Galerkin approximation of $u \in L^2(\Gamma)$. Denote by z and $z^{(h)}$ the corresponding points in the numerical range of $A_{k,\eta}$ given by*

$$z := \frac{\langle A_{k,\eta}u, u \rangle}{\langle u, u \rangle}, \quad z^{(h)} := \frac{\langle A_{k,\eta}u^{(h)}, u^{(h)} \rangle}{\langle u^{(h)}, u^{(h)} \rangle}$$

Then there exists h_0 such that for all $h \leq h_0$ we have

$$|z - z^{(h)}| \leq Ch^2 \tag{4.10}$$

for some $C > 0$ independent of u and h .

Proof. Splitting up $A_{k,\eta}$ into A_H and A_S as defined in Lemma 4.8 gives

$$z = \frac{\langle A_H u, u \rangle}{\langle u, u \rangle} + i \frac{\langle A_S u, u \rangle}{\langle u, u \rangle}$$

From Lemma 4.8 it follows that Lemma 4.6 can be applied separately to the real and imaginary parts of z and $z^{(h)}$ resulting in (4.10). \square

By using the approximation result (4.10) in the proof of Theorem 4.4 we immediately obtain the following $O(h^2)$ convergence result for the numerical range of the operator $A_{k,\eta}$.

THEOREM 4.10. *Let the assumptions of Lemma 4.9 hold. Then for any $\epsilon > 0$ there exists $C > 0$, which depends on $A_{k,\eta}$ and ϵ such that $W(A_{k,\eta}^{(h)}) \subset W(A_{k,\eta}) + \Delta_{Ch^2}$ and*

$$W_\epsilon(A) \subset W(A_{k,\eta}^{(h)}) + \Delta_{Ch^2}.$$

5. Numerical examples. In this section we demonstrate the convergence of the numerical range and the coercivity constant as $h \rightarrow 0$ and apply the numerical range computation to test the coercivity of the integral operator A for several interesting domains. For simplicity, we take the most commonly used choice of coupling constant, $\eta = k$ and omit the indices in $A_{k,\eta}$ since the k -dependence is clear from the context.

5.1. Convergence of the numerical range as $h \rightarrow 0$. We start by demonstrating the convergence results of Section 4.2. Consider the operator A on the unit circle with $k = 1$. For the BEM discretisation we decompose the unit circle into elements of equal length h and choose piecewise constant basis functions on each element. From Theorem 4.10 it follows that the convergence of the numerical range is at least quadratic. We approximate the numerical range of $A^{(h)}$ with the exterior approximation algorithm described in Section 4.1 using 50 eigenvalue computations, resulting in an approximating polygon with 100 corners. An approximation for the coercivity constant $\gamma^{(h)}$ of $A^{(h)}$ is then given as the distance of the exterior polygon to the origin. The rate of convergence for decreasing h is shown in Figure 5.1. For smooth domains, such as the circle, with boundary length L we use approximately $\frac{NLk}{2\pi}$ elements, that is $h \approx \frac{2\pi}{Nk}$. For polygonal domains, considered later, L is the length of a boundary segment. Hence, h can differ on each segment. With this notation $N = 10$ corresponds to the rule of thumb of 10 elements per wavelength. The error for the coercivity constant of the circle is measured as $|\gamma^{(h)} - 1|$ since it is known that for sufficiently large k the exact coercivity constant is 1. Indeed, the convergence curve seems to confirm this result for the wavenumber $k = 1$.

With piecewise constant basis functions the convergence is approximately quadratic as predicted. At an accuracy of around 10^{-4} it starts slowing down. We suspect that this is due to the limit in accuracy given by the polygonal approximation of the numerical range. For comparison we also give the rate of convergence using piecewise quadratic basis functions. Already with 10 elements per wavelength the approximate coercivity constant has an error of less than 1%.

We now consider the approximation of the coercivity constant of A on the unit square. Again, we choose $k = 1$. The convergence of the coercivity constant for approximations with piecewise constant basis functions is shown in the upper left plot of Figure 5.2 (square-dotted line). The observed convergence is much slower than the expected maximum asymptotic rate of $O(h)$ from Theorem 4.4. The reason is shown in the upper right plot of Figure 5.2. It shows the logarithmic plot of a boundary function that is associated with a point in the numerical range close to 0.5. It was computed as an eigenfunction of a Galerkin discretisation of A with piecewise quadratic basis functions and exponential h -refinement towards the corners. It has a large $H^1(\Gamma)$ norm, indicating that the constants of the estimate in Theorem 4.4 will become large for $\alpha = 1$. Hence, this function is much better represented as a function in $H^\alpha(\Gamma)$ for some $\alpha < 1$ and we expect the visible numerical rate of convergence to be $O(h^\alpha)$, even though eventually the asymptotic rate will approach $O(h)$. The lower left plot of Figure 5.2 shows the effect on the shape of the numerical range. With $N = 2000$, that is roughly 2000 elements per wavelength, the numerical range of

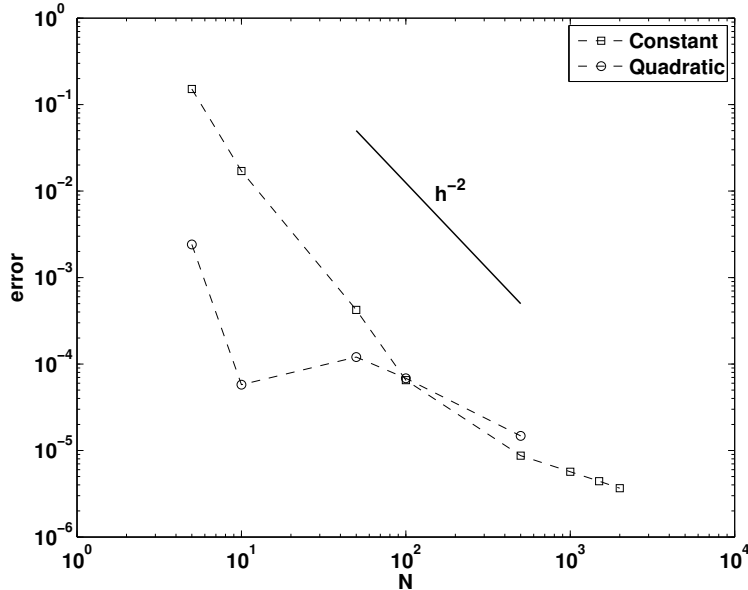


Fig. 5.1: Convergence of the coercivity constant for a growing number of elements per wavelength on the unit circle for $k = 1$ with linear and quadratic basis functions.

the discretisation only fills parts of the exact numerical range, leading to an overestimation of the coercivity constant. The (up to plotting accuracy) correct numerical range was obtained by using piecewise quadratic basis functions together with exponential h -refinement towards corners. The lower right plot shows the approximate spectrum (black dots) and the boundary of the numerical range obtained with this strategy. The convergence of the coercivity constant $\gamma^{(h)}$ for the refined discretisations is shown as the circle-dotted line in the upper left plot of Figure 5.2. N means here that approximately N elements per wavelength were used until a distance of $\frac{2\pi}{Nk}$ away from the corner together with exponential h -refinement in the direct neighbourhood around the corner. This gives an accuracy of around 10^{-2} for $N = 10$. The best obtained value for the coercivity constant on the square is 0.318 using $N = 3000$. As comparison for $N = 10$ we obtain 0.329, a relative distance of less than 4% to the best value. On the plotting scale there is no significant difference between the numerical range for $N = 10$ and for $N = 3000$ using the exponential refinement close to the corners.

5.2. Numerical range and coercivity constant for growing k . In this section we numerically investigate the behavior of the numerical range and the coercivity constant for growing wavenumber k of the integral operator A for the boundaries of several polygonal and smooth domains.

For smooth domains we used BEM discretisations with piecewise quadratic basis functions and for cornered domains we additionally applied exponential h -refinement towards the corners. Typically we used between 10 and 20 elements per wavelength away from the corners depending on the overall system size. Whenever possible within the limit of the available memory and feasible computing times we checked the accuracy by refining h . At least on the level of plotting accuracy we always found good agreement between the results for 10 elements per wavelength and higher values for the number of elements. All computations were done using a self-developed C++ code, which is OpenMP parallelized. It ran on an 8 core Linux workstation with 64GB RAM. The finest discretisations that were still feasible in terms of computing time led to matrix problems of dimensions between ten and eleven thousand. Since 50 eigenvalue decompositions of the Hermitian part of complex rotations of the operator needed to be performed to obtain an approximating polygon for the numerical range with 100 corners, the overall computing time

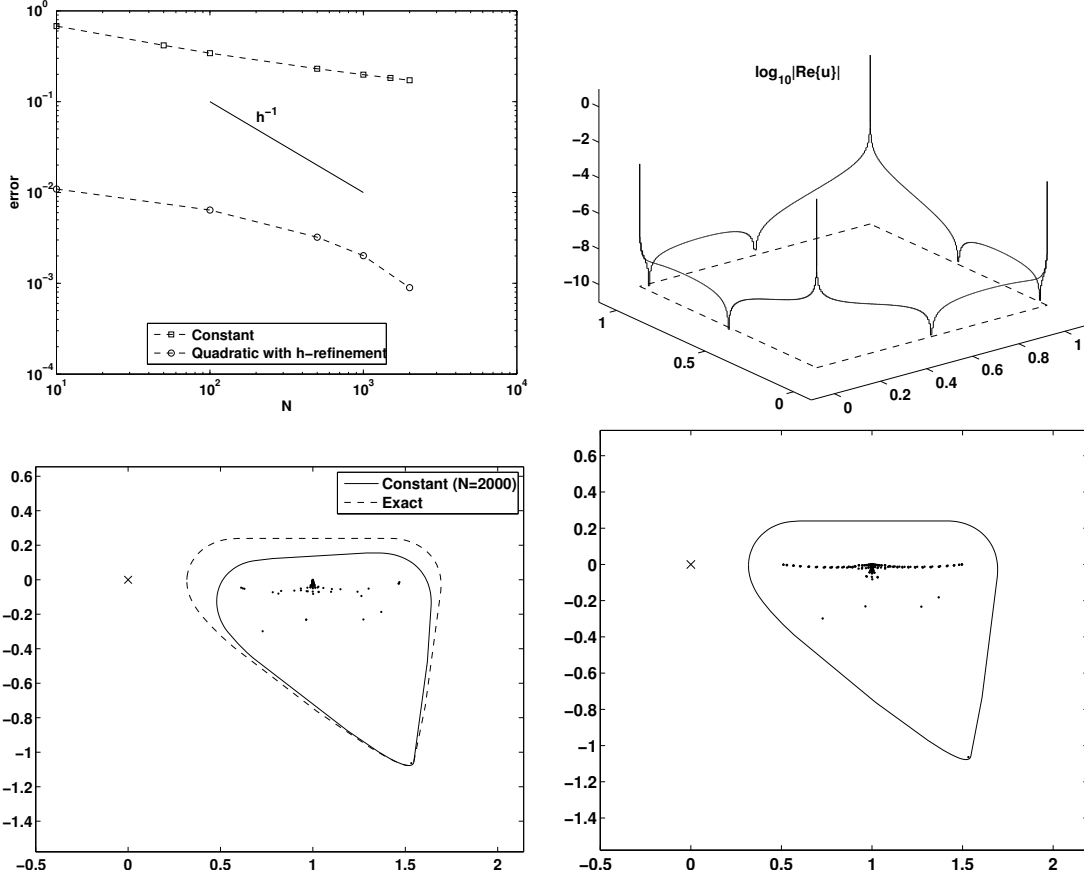


Fig. 5.2: Upper left:) Rate of convergence of $\gamma^{(h)}$ on the unit square. Upper right:) A function associated with a point of the numerical range close to 0.5 . Lower left:) Approximate numerical range using piecewise constant basis functions (solid line) against exact numerical range (dotted line). The dots show the eigenvalues of the Galerkin projection $A^{(h)}$. Lower right:) Approximation to exact numerical range and the spectrum of A on the square obtained by using piecewise quadratic basis functions and h-refinement towards corners of the square.

was roughly in the range of 12 to 20 hours for the largest matrix problems. Due to the cubic dependence of the computing time for the full matrix problems on the dimension of the matrices, doubling the number of elements leads to an additional factor 8 in time.

5.2.1. Smooth domains. For the unit circle coercivity was already shown for sufficiently large k in [18]. Therefore, we are more interested for this domains in what happens as $k \rightarrow 0$. The corresponding values of the coercivity constant γ are given in the following table.

k	0.01	0.1	1	10
γ	0.01	0.57	1.00	1.00

For $k = 1$ and above the coercivity constant indeed seems to be 1. However, as $k \rightarrow 0$ the numerical range starts deteriorating into a line and it appears that also $\gamma \rightarrow 0$. This is consistent with the fact that the choice $\eta = k$ is not optimal for small wavenumbers (see Section 2), and also with the fact that $A_0 = I + K'_0$ is not invertible, and hence not coercive, on $L^2(\Gamma)$ for any Lipschitz domain since it maps any L^2 function into one with zero mean and hence is not surjective [38]. However, if we fix $\eta = 1$, then for $k = 0.1$ and $k = 0.01$ we obtain that the coercivity constant is 1. Since the

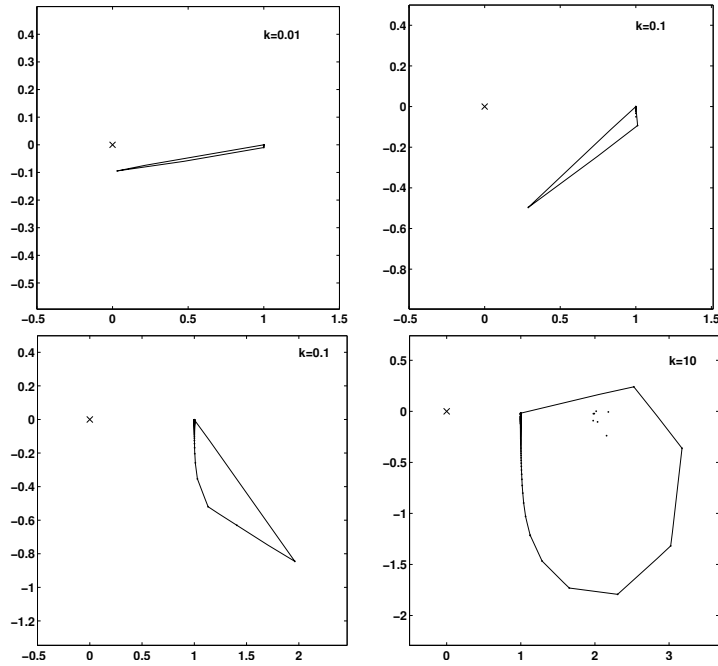


Fig. 5.3: The numerical range of A on the unit circle for $k = 0.01, 0.1, 1, 10$. The black dots are approximations to the spectral values of A .

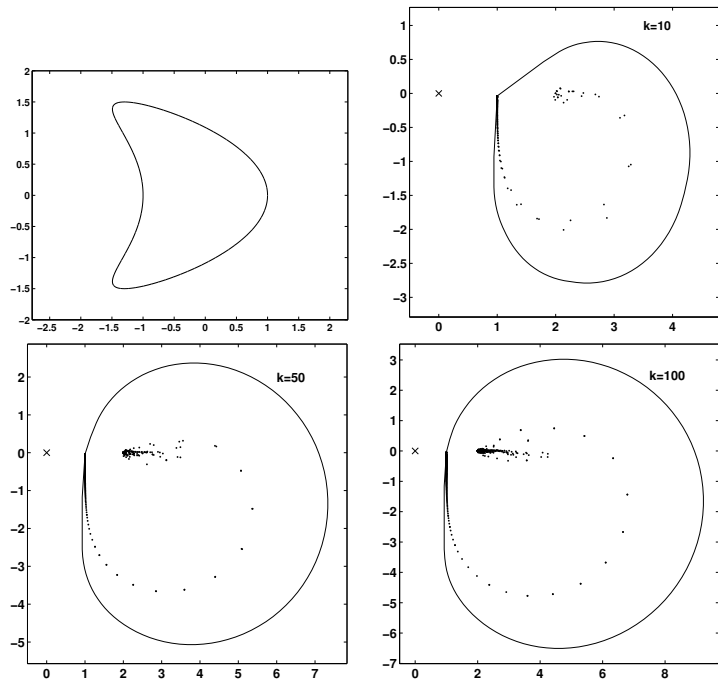


Fig. 5.4: The numerical range of A on a kite shape (upper left plot) for $k = 10, 50, 100$.

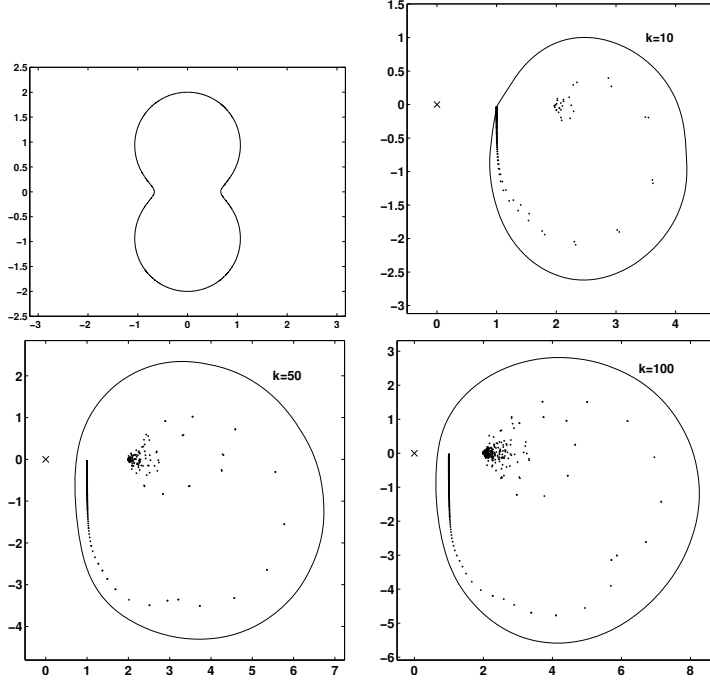


Fig. 5.5: An inverted ellipse and the associate numerical range of A for $k = 10, 50, 100$.

eigenvalues of A on the unit circle are explicitly known (see for example [18]) and the numerical range is just the convex hull of the spectrum in this case one may also approximate the coercivity constant for the unit circle directly without using a Galerkin discretization of the operator. Also, it is interesting to note that for growing k more and more eigenvalues cluster around the point 2 (see Figure 3.1). However, for each k there can only be a finite number of eigenvalues close to 2 since A on the unit circle is a compact perturbation of the identity and therefore the only accumulation point of the eigenvalues is 1.

The next domain is a kite shape. A parameterization of its boundary is given by $Z(t) = \cos t + 0.65 \cos 2t - 0.65 + 1.5i \sin t$, $t \in [0, 2\pi]$. The numerical range for $k = 10, 50, 100$ is shown in Figure 5.4. Again, as in the case of the unit circle there are more and more eigenvalues appearing close to 2 as k becomes larger. However, the main difference between this domain and the circle is that the operator A is not normal since the numerical range is not just the convex hull of the eigenvalues. But interestingly we still have $\gamma \approx 1$ for all three cases. Again, the coercivity constant seems to be independent of the wavenumber for sufficiently large k . The size of the numerical range grows as k becomes larger. This is due to the norm bound (2.5) and the equivalence of the numerical radius and the norm of A in (3.4).

In the next example we show results for a domain, which like the kite is nonconvex and star-shaped but for which the coercivity constant of A shows a very different behaviour for growing k . It is an inverted ellipse defined by $Z(t) = \frac{e^{it}}{1 + \frac{1}{2}e^{2it}}$, $t \in [0, 2\pi]$. The inverted ellipse and the corresponding numerical range of A for $k = 10, 50, 100$ are shown in Figure 5.5. The following table shows approximations of the coercivity constant γ for the different wavenumbers.

k	10	50	100	200
γ	0.988	0.737	0.672	0.585

It is striking that in contrast to the circle and the kite shape γ does not seem to be independent of k . It is an open question whether there is a lower bound $C > 0$, such that $\gamma > C$ for all k on

the inverted ellipse or whether $\gamma \rightarrow 0$ as $k \rightarrow \infty$ (see also the discussion in Section 6).

5.2.2. Polygonal domains. We start with two simple convex polygons, namely the unit square and the equilateral triangle. For the unit square and $k = 1$ a plot of the numerical range was already shown in Figure 5.2. We now present results for growing k . Figure 5.6 shows the numerical range and approximations of the spectra for A on the square in the case of the wavenumbers $k = 10, 50, 100$. The lower right plot shows a comparison of the numerical range in all three cases. Again, due to (2.6) and (3.4) the size of the numerical range grows for growing k . For γ we obtain in all three cases the approximation $\gamma \approx 0.328$. It is interesting to note that close to the origin for all three wavenumbers the boundary of the numerical range is almost identical (see the lower right plot of Figure 5.6). For $k = 1$ we computed a value of $\gamma \approx 0.318$ using approximately 3000 elements per wavelength while here we used around 20 elements per wavelength. Hence, the value of γ for the higher wavenumbers has a relative distance of around 3% to the value for $k = 1$, which is likely due to the higher discretisation error (note that for 10 elements per wavelength we reported a value of 0.329 in Section 5.1).

As Figure 5.7 shows the operator A on the equilateral triangle has a very similar behaviour. Again, the computed coercivity constant does not seem to change in dependence on the wavenumber. For the three considered wavenumbers $k = 10, 50, 100$ we have $\gamma \approx 0.17$.

The square and the triangle are both convex domains, and both exhibit numerical wavenumber independence of γ . To see that this feature is not restricted to convex polygonal domains consider the L-Shape in Figure 5.8. Again, the coercivity constant seems to be independent of the wavenumber with a value of $\gamma \approx 0.30$. Figure 5.9 shows the results for a polygon which is not only non-convex, but is also non-star-shaped, and again the results are very similar to the other domains. In this example we have $\gamma \approx 0.30$ for all three wavenumbers, which interestingly is, up to numerical accuracy, identical to the value for the L-Shape.

5.3. A trapping domain. Our last example is the trapping domain shown in Figure 5.10, so-called because the open cavity can “trap” high frequency waves. That is, we expect there to be asymptotically trapped modes of the PDE (1.5) in the cavity for large wavenumbers k that are multiples of 5 (since the width of the cavity is $\pi/5$). This fact was used in [13] to show that for this domain $\|A^{-1}\|$ satisfies (2.4) for k_n multiples of 5, and hence the operator A cannot be uniformly coercive for large k . Figure 5.11 shows the numerical range of A for this domain in the cases $k = 4, 5, 8, 10$. For $k = 4$ and $k = 8$ the operator A is coercive. But for $k = 5$ and $k = 10$ we lose coercivity. These numerical results seem to indicate that the loss of coercivity is closely connected to the nonnormality of the operator: for all wavenumbers in Figure 5.11 the spectrum of A is in the right-half plane independent of whether the operator is coercive or not. This again suggests that spectral information is not sufficient to understand coercivity. We now give a possible explanation for the loss of coercivity at $k = 5$ and $k = 10$ by considering resonances of the exterior scattering problem. A resonance (or scattering pole) can be defined as a wavenumber k_{res} , for which there exists a sequence $u^{(n)} \in L^2(\Gamma)$, $\|u^{(n)}\| = 1$, satisfying

$$\|Au^{(n)}\| \rightarrow 0$$

as $n \rightarrow \infty$, that is $\|A^{-1}\|$ is infinite (see Remark 5.2). For $\text{Im}\{k\} \geq 0$ this is not possible as in this case A is bijective on $L^2(\Gamma)$ (the proof of this for $k \in \mathbb{R}$ in [14] can easily be extended to the case $\text{Im}\{k\} > 0$). Hence, any resonances can only be in the lower half-plane.

If a resonance k_{res} is close to the real axis we expect that solutions of the soundsoft scattering problem for real wavenumbers close to k_{res} will be affected since $\|A^{-1}\|$ will still be large for k sufficiently close to the resonance. However the coercivity of the operator may be also affected as the following Theorem shows.

THEOREM 5.1. *Let $k_{res} \in \mathbb{C}$, $\text{Im}\{k_{res}\} < 0$, be a resonance. Then $A_{k_{res}, \eta}$ is not coercive for this wavenumber.*

Proof. If k_{res} is a resonance then by definition there exists a sequence $u^{(n)}$, $\|u^{(n)}\| = 1$, such that $\|A_{k_{res}, \eta} u^{(n)}\| \rightarrow 0$ for $n \rightarrow \infty$. It follows that $\langle A_{k_{res}, \eta} u^{(n)}, u^{(n)} \rangle \rightarrow 0$. Hence, $A_{k_{res}, \eta}$ is not coercive. \square

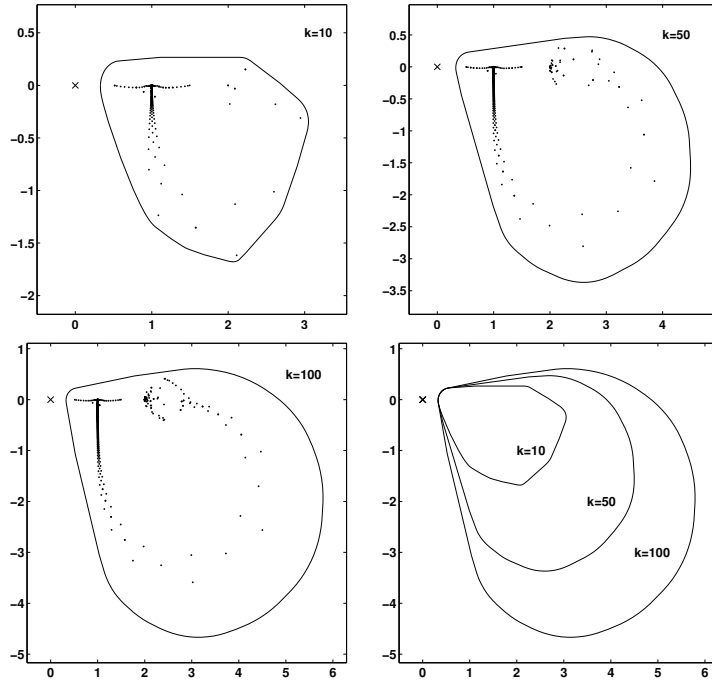


Fig. 5.6: The numerical range of A on the unit square for $k = 10, 50, 100$. The black dots are approximations to the spectral values of A . The lower right plot shows a comparison of the numerical ranges for the three different wavenumbers.

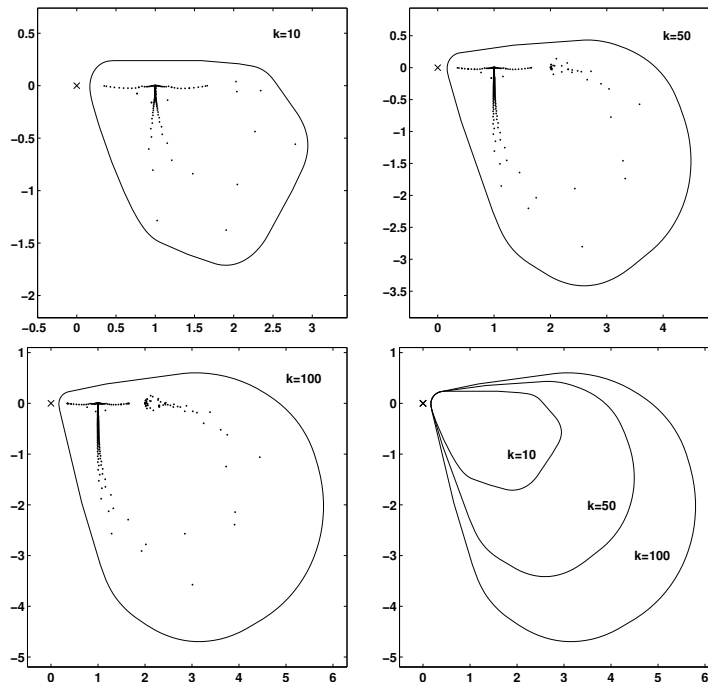


Fig. 5.7: The numerical range of A on the equilateral triangle with sides of unit length for $k = 10, 50, 100$.

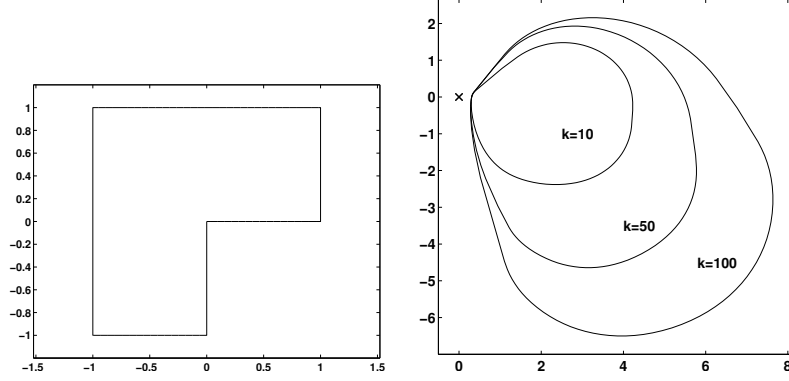


Fig. 5.8: The numerical range for $k = 10, 50, 100$ of A for the L-shaped domain.

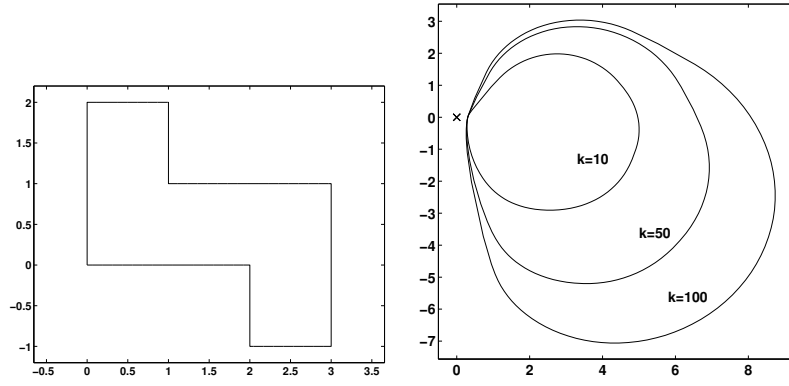


Fig. 5.9: The numerical range for $k = 10, 50, 100$ of A for a non-starshaped domain (“double-L”).

If 0 is in the interior of the numerical range $W(A)$ for a resonance k_{res} then by continuity there exists a neighbourhood of k_{res} , such that A is not coercive for any wavenumber k in this neighbourhood.

In Figure 5.12 we show a contour plot of $\log_{10}(\|A\|^{-1})$ in the case of the trapping domain over a part of the negative half of the complex plane. Three resonances in the negative half of the complex plane are visible in this plot. We also computed the numerical range for k in the interval from 4 to 12 to obtain estimates for which real wavenumbers the operator A loses coercivity. The corresponding ranges are shown as dashed lines in Figure 5.12. Note that the coercivity statements are with respect to the corresponding real wavenumbers.

REMARK 5.2. *Resonances, or scattering poles, are fundamental objects in the study of scattering theory. A nice introduction to this area is given in [36, Chapter 7], but we sketch a brief outline below. Consider the scattered field u_s for the acoustic scattering problem: this satisfies the Helmholtz equation (1.5), the radiation condition (1.7), and a Dirichlet boundary condition which we shall write as*

$$u_s = f \quad \text{on } \partial\Omega.$$

We can then abstractly write

$$u_s = B_k f$$

where B_k is the solution operator, where the subscript emphasises the k -dependence. B_k is a uniquely defined operator-valued function of k for $\text{Im}\{k\} \geq 0$, and analytic for $\text{Im}\{k\} > 0$. In

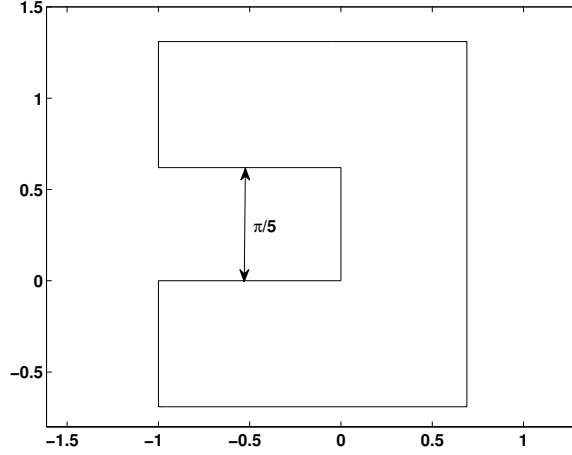


Fig. 5.10: A trapping domain. The open cavity has a width of $\pi/5$.

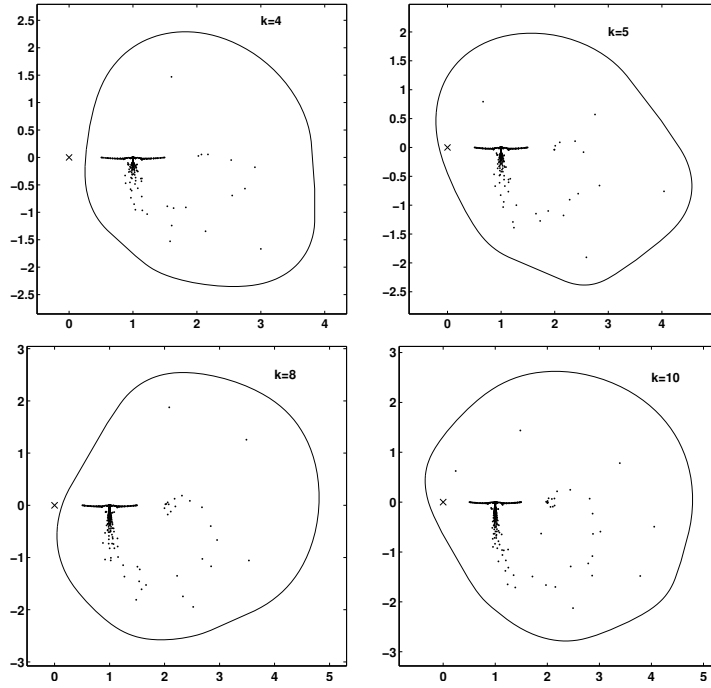
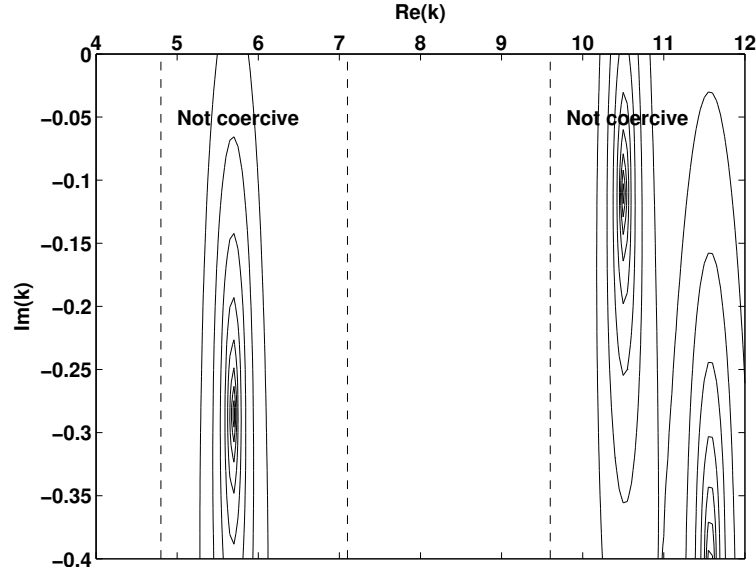


Fig. 5.11: The numerical range of A for the trapping domain from Figure 5.10 in the cases $k = 4, 5, 8, 10$.

fact, B_k can be analytically continued into $\text{Im}\{k\} < 0$ except for certain poles, and these are called the “resonances” or “scattering poles”. When k is one of these scattering poles, there exists an outgoing solution of (1.5) which is zero on $\partial\Omega$, where a function v is called outgoing if

$$v \sim C \frac{e^{ikr}}{r^{(d-1)/2}} \text{ as } r \rightarrow \infty,$$

where C depends only on the angular variables and d is the dimension. However outgoing solutions with k having negative imaginary part grow exponentially towards infinity and do not satisfy the Sommerfeld radiation condition (1.7).



5.12

Fig. 5.12: Contour plot of $\log_{10}(\|A^{-1}\|)$ over a part of the complex plane. The dashed lines show ranges, where for k on the real axis the operator A is not coercive.

	Smooth	Polygonal
Convex	Circle –coercive, uniform in k	Square –coercive, uniform in k Equilateral triangle –coercive, uniform in k
Non-convex, star-shaped	Kite –coercive, uniform in k Inverted ellipse –coercive, not uniform in k	L-shaped –coercive, uniform in k
Non-star-shaped		Double-L –coercive, uniform in k Trapping –coercivity depends on k

Table 6.1: Summary of the numerical results on coercivity of the operator A on various domains for $k = 10, 50, 100$.

In a neighborhood of the positive real k axis, B_k can be expressed in terms of the boundary integral operator A'_k , equation (2.1), as follows:

$$B_k = 2(\mathcal{D}_k - i\eta\mathcal{S}_k)(A'_k)^{-1} \quad (5.1)$$

where the double- and single-layer potentials are defined by

$$\mathcal{D}_k u(x) := \int_{\Gamma} \frac{\partial \Phi(x, y)}{\partial n(y)} u(y) ds(y), \quad \mathcal{S}_k u(x) := \int_{\Gamma} \Phi(x, y) u(y) ds(y), \quad x \in \mathbb{R}^2 \setminus \Gamma$$

$\eta \in \mathbb{R}^+ \setminus \{0\}$, and the subscripts again emphasise the k -dependence, [36, equation (7.32)]. This representation of B_k shows that, in the neighborhood of \mathbb{R}^+ where this formula is valid, the scattering poles are equal to the poles of $(A'_k)^{-1}$, and hence to the poles of A_k^{-1} (using the fact that $\|(A'_k)^{-1}\| = \|A_k^{-1}\|$ [15]). The scattering poles, as defined above, are also equal to the poles of the so-called “scattering operators” for both the acoustic scattering problem and the time-dependent wave equation [36, Chapter 7].

6. Conclusions. Coercivity is still a largely open problem for boundary integral formulations of acoustic scattering problems. In this paper we used the close connection to the numerical range

of the operator to investigate coercivity on several interesting domains in two dimensions. The numerical results demonstrate that coercivity of the direct combined boundary integral operator A seems to hold uniformly on a wide range of domains. This is surprising since for standard domain based variational formulations of the underlying Helmholtz equation only a weaker Gårding inequality, with k dependent perturbation term, holds [23]. Table 6.1 summarizes the results for the different domains. Coercivity seems to hold uniformly (with respect to the numerical accuracy of the results) and independently of the wavenumber for all considered domains apart from the inverted ellipse and the trapping domain. For the inverted ellipse it is not clear from the current results whether $\gamma \rightarrow 0$ as $k \rightarrow \infty$ or whether there exists a lower bound C , such that $C < \gamma$ for all sufficiently large k . The trapping domain behaves very differently from the other domains, and we saw that the boundary integral operator has resonances close to the real axis which helped explain why it is not coercive. This leads us to make the following conjecture:

CONJECTURE 6.1. *The combined boundary integral operator A is coercive on bounded domains for all wavenumbers k that are sufficiently far away from a resonance.*

The fact that the trapping domain behaves so differently from the other domains considered here is not surprising. Indeed, in scattering theory for the time dependent wave equation, the geometry of the domain, and in particular whether it is trapping or not, plays a key role [27]. Recall the definition of “trapping” and “non-trapping” from the epilogue of [27]: consider all the rays starting in the exterior of Ω inside some large ball of finite radius. Continue all the rays according to the law of reflection (angle of incidence equals angle of reflection) whenever they hit $\partial\Omega$, until they finally leave the large ball. We call Ω trapping if there are arbitrary long paths or closed paths of this kind; otherwise Ω is non-trapping. (Note that there are subtleties associated with rays hitting the boundary at a tangent, and also for domains with non-smooth boundaries.)

The connection between whether a domain is trapping or not and the location of resonances is a classic problem: in the 1967 first edition of [27], Lax and Philips conjectured that

1. for a non-trapping domain there are no resonances in a strip $\{k : \text{Im}\{k\} \leq \alpha\}$ for some constant $\alpha > 0$, and
2. for a trapping domain there is a sequence of resonances $\{k_j\}_{j=1}^{\infty}$ such that $\text{Im}\{k_j\} \rightarrow 0$ as $j \rightarrow \infty$.

The first statement was proved to be correct in [31] and [30]; however examples of trapping domains for which there are no resonances in a strip below the real axis were given in [6], [24], and thus the second statement is incorrect. (More details about these results are given in [27, Epilogue].)

Returning to the question of coercivity, the result 1 above implies that for the inverted ellipse there are no resonances in a strip below the imaginary axis, lending support to the idea that coercivity is uniform for higher k . Combining Conjecture 6.1 with the result 1, leads to the following conjecture:

CONJECTURE 6.2. *The combined boundary integral operator A is coercive uniformly in k , for all sufficiently large wavenumbers k , for all non-trapping domains.* (This obvious depends on whether the strip in result 1 causes the resonances to be “sufficiently far away” from the real axis, however there are some results which say that the resonances increase in distance from the real axis as k increases [27, Epilogue].)

Note that, as mentioned in Section 2, for a certain class of trapping domains (including the domain considered in Section 5.3) A has already been proven not to be uniformly coercive in k , however still much work has to be done to establish whether these conjectures are true or not. In particular, the connection between resonances/trapping and coercivity needs to be more closely investigated.

Apart from investigating coercivity itself, this paper points to several other open research directions. We did not discuss the plots of the spectra in detail, but nevertheless they show some interesting features, especially for the polygonal domains where the operator is not a compact perturbation of the identity. In addition the connection to nonnormality should be investigated further: it appears that the operator is nonnormal for all domains other than the unit circle, and it would be interesting if this could be proved. It seems that coercivity is intimately linked to this nonnormality: indeed, as the example of the trapping domain shows, spectral information appears to be largely irrelevant for answering the question of whether coercivity holds or not. However,

the behaviour of nonnormal matrices and operators is still an open problem in many applications (see the book by Trefethen and Embree [37]).

Finally, with this paper we would like to advertise the use of the numerical range and related concepts like pseudospectra [37] for investigating the properties of boundary integral operators. Many interesting results can be expressed in terms of the numerical range such as the reformulation of Céa's Lemma in Theorem 3.7, and estimates for iterative solvers [19, 20].

Acknowledgements. Both authors would like to thank Ivan Graham (Bath) and Simon Chandler-Wilde (Reading) for helpful discussions that improved the paper. The first author would also like to thank Ivan Graham for an invitation to Bath in November 2009, which started this paper.

REFERENCES

- [1] M. ABRAMOWITZ AND I. A. STEGUN, *Handbook of mathematical functions: with formulas, graphs, and mathematical tables*, Courier Dover Publications, 1965.
- [2] S. AMINI, *On the choice of the coupling parameter in boundary integral formulations of the exterior acoustic problem*, *Applicable analysis*, 35 (1990), pp. 75–92.
- [3] ———, *Boundary integral solution of the exterior acoustic problem*, *Comput. Mech*, 13 (1993), pp. 2–11.
- [4] K. ATKINSON, *The numerical solution of integral equations of the second kind. 1997*, Cambridge Monographs on Applied and Computational Mathematics, (1997).
- [5] L. BANJAI AND S. SAUTER, *A refined Galerkin error and stability analysis for highly indefinite variational problems*, *SIAM Journal on Numerical Analysis*, 45 (2008), pp. 37–53.
- [6] C. BARDOS, J. GUILLOT, AND J. RALSTON, *La relation de possion pour l'equation des ondes dans un ouvert non borne application a la theorie de la diffusion*, *Communications in Partial Differential Equations*, 7 (1982), pp. 905–958.
- [7] T. BRACONNIER AND N. J. HIGHAM, *Computing the field of values and pseudospectra using the Lanczos method with continuation*, *BIT*, 36 (1996), pp. 422–440.
- [8] H. BRAKHAGE AND P. WERNER, *Über das dirichletsche Aussenraumproblem für die Helmholtzsche Schwingungsgleichung*, *Archiv der Mathematik*, 16 (1965), pp. 325–329.
- [9] S. C. BRENNER AND L. R. SCOTT, *The mathematical theory of finite element methods*, vol. 15 of Texts in Applied Mathematics, Springer, New York, second ed., 2002.
- [10] O. P. BRUNO AND L. A. KUNYANSKY, *Surface scattering in three dimensions: an accelerated high-order solver*, *Proceedings: Mathematics, Physical and Engineering Sciences*, (2001), pp. 2921–2934.
- [11] J. V. BURKE AND A. GREENBAUM, *Characterizations of the polynomial numerical hull of degree k*, *Linear Algebra and its Applications*, 419 (2006), pp. 37 – 47.
- [12] S. N. CHANDLER-WILDE AND I. G. GRAHAM, *Boundary integral methods in high frequency scattering*, in *Highly Oscillatory Problems: Computation, Theory and Applications*, B. Engquist, T. Fokas, E. Hairer, and A. Iserles, eds., Cambridge University Press, 2009.
- [13] S. N. CHANDLER-WILDE, I. G. GRAHAM, S. LANGDON, AND M. LINDNER, *Condition number estimates for combined potential boundary integral operators in acoustic scattering*, *Journal of Integral Equations and Applications*, 21 (2009), pp. 229–279.
- [14] S. N. CHANDLER-WILDE AND S. LANGDON, *A Galerkin boundary element method for high frequency scattering by convex polygons*, *SIAM J. Numer. Anal.*, 45 (2007), pp. 610–640.
- [15] S. N. CHANDLER-WILDE AND P. MONK, *Wave-number-explicit bounds in time-harmonic scattering*, *SIAM J. Math. Anal.*, 39 (2008), pp. 1428–1455.
- [16] D. L. COLTON AND R. KRESS, *Integral equation methods in scattering theory*, Pure and Applied Mathematics (New York), John Wiley & Sons Inc., New York, 1983. A Wiley-Interscience Publication.
- [17] D. L. COLTON AND R. KRESS, *Inverse acoustic and electromagnetic scattering theory*, Springer Verlag, 1998.
- [18] V. DOMÍNGUEZ, I. G. GRAHAM, AND V. P. SMYSHLYAEV, *A hybrid numerical-asymptotic boundary integral method for high-frequency acoustic scattering*, *Numer. Math.*, 106 (2007), pp. 471–510.
- [19] T. A. DRISCOLL, K.-C. TOH, AND L. N. TREFETHEN, *From potential theory to matrix iterations in six steps*, *SIAM Review*, 40 (1998), pp. 547–578.
- [20] M. EMBREE, *How descriptive are GMRES convergence bounds?*, Tech. Rep. 99/08, Oxford University Computing Laboratory, 1999.
- [21] K. GIEBERMANN, *Schnelle Summationsverfahren zur numerischen Lösung von Integralgleichungen für Streuprobleme im R3*, PhD thesis, University of Karlsruhe, 1997.
- [22] K. E. GUSTAFSON AND D. K. M. RAO, *Numerical range; The field of values of linear operators and matrices*, Universitext, Springer-Verlag, New York, 1997.
- [23] F. IHLENBURG, *Finite element analysis of acoustic scattering*, vol. 132 of Applied Mathematical Sciences, Springer-Verlag, New York, 1998.
- [24] M. IKAWA, *On the poles of the scattering matrix for two strictly convex obstacles*, *J. Math. Kyoto Univ*, 23 (1983), pp. 127–194.
- [25] R. KRESS, *Minimizing the condition number of boundary integral operators in acoustic and electromagnetic scattering*, *The Quarterly Journal of Mechanics and Applied Mathematics*, 38 (1985), p. 323.

- [26] R. KRESS AND W. T. SPASSOV, *On the condition number of boundary integral operators in acoustic and electromagnetic scattering*, Numerisch Mathematik, 42 (1983), pp. 77–95.
- [27] P. LAX AND R. PHILLIPS, *Scattering theory*, Academic Press, revised ed., 1989.
- [28] R. LEIS, *Zur Dirichletschen Randwertaufgabe des aussenraumes der schwingungsgleichung*, Mathematische Zeitschrift, 90 (1965), pp. 205–211.
- [29] W. C. H. MCLEAN, *Strongly elliptic systems and boundary integral equations*, Cambridge Univ Pr, 2000.
- [30] R. MELROSE, *Singularities and energy decay in acoustical scattering*, Duke Math. J, 46 (1979), pp. 43–59.
- [31] C. MORAWETZ, J. RALSTON, AND W. STRAUSS, *Decay of solutions of the wave equation outside nontrapping obstacles*, Comm. Pure Appl. Math, 30 (1977), pp. 447–508.
- [32] P. MORSE AND H. FESHBACH, *Methods of theoretical physics. Vol. I. II*, New York, (1953).
- [33] O. I. PANIČ, *On the question of the solvability of the exterior-value problems for the wave equation and Maxwell's equations*, Usp. Mat. Nauk, 20A (1965), pp. 221–226.
- [34] I. H. SLOAN AND A. SPENCE, *The Galerkin method for integral equations of the first kind with logarithmic kernel: Theory*, IMA journal of numerical analysis, 8 (1988), p. 105.
- [35] O. STEINBACH, *Numerical approximation methods for elliptic boundary value problems*, Springer, New York, 2008. Finite and boundary elements, Translated from the 2003 German original.
- [36] M. TAYLOR, *Partial differential equations II, Qualitative studies of linear equations, volume 116 of Applied Mathematical Sciences*, Springer-Verlag, New York, 1996.
- [37] L. N. TREFETHEN AND M. EMBREE, *Spectra and pseudospectra*, Princeton University Press, Princeton, NJ, 2005.
- [38] G. VERCHOTA, *Layer potentials and regularity for the Dirichlet problem for Laplace's equation in Lipschitz domains*, Journal of Functional Analysis, 59 (1984), pp. 572–611.